UCRL-JC-131566
PREPRINT

Equations of State of Unreacted High Explosives at High Pressures

C-S. Yoo
H. Cynn
W.M. Howard
N. Holmes

This paper was prepared for submittal to the
11th International Detonation Symposium
Snowmass Village, CO
August 31-September 4, 1998

August 14, 1998

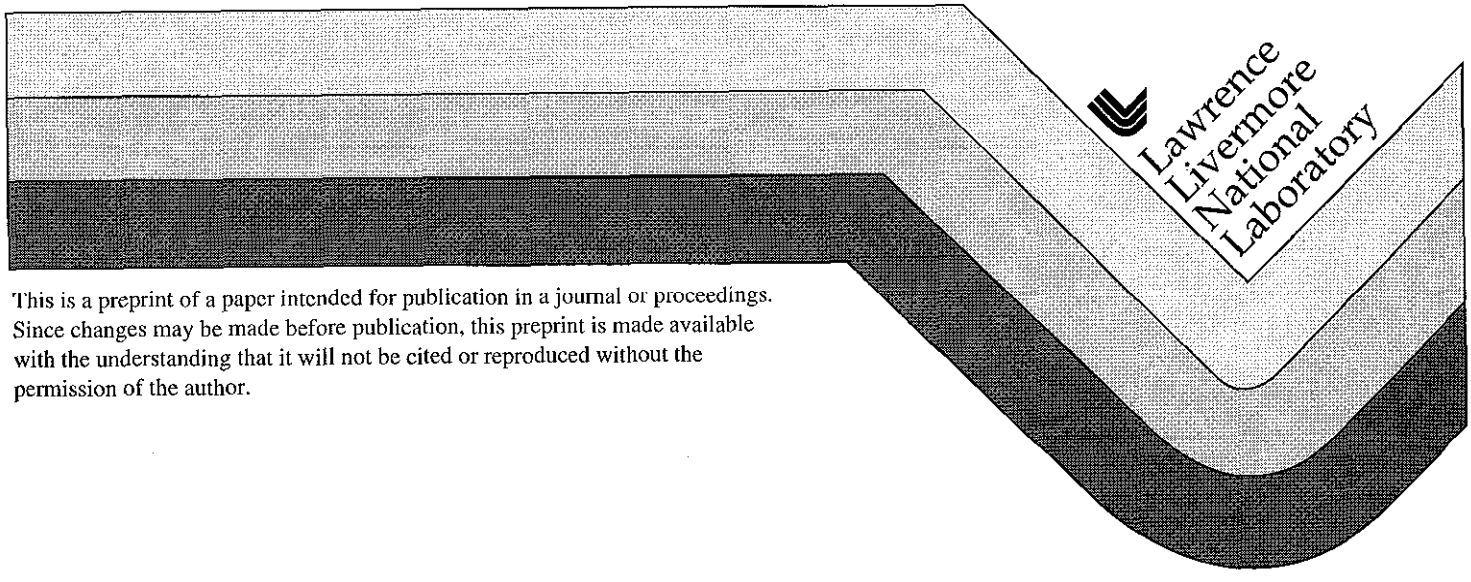

EQUATIONS OF STATE OF UNREACTED HIGH EXPLOSIVES AT HIGH PRESSURES

Choong-Shik Yoo, Hyunchae Cynn, W. Michael Howard, Neil Holmes
Lawrence Livermore National Laboratory
P.O. Box 808, Livermore, CA94550

Isotherms of unreacted high explosives (HMX, RDX, and PETN) have been determined to quasi-hydrostatic high pressures below 45 GPa, by using a diamond-anvil cell angle-resolved synchrotron x-ray diffraction method. The equation-of-state parameters (bulk modulus B_o and its derivatives B') are presented for the 3rd-order Birch-Murnaghan formula based on the measured isotherms. The results are also used to retrieve unreacted Hugoniots in these high explosives and to develop the equations of state and kinetic models for composite high explolsives such as XTX-8003 and LX-04. The evidence of shear-induced chemistry of HMX in non-hydrostatic conditions is also presented.

INTRODUCTION

High-pressure equation-of-state (EOS) information of high explosives (HE's) is fundamental to understand intermolecular interactions of energetic molecules and is therefore needed for thermochemical descriptions of various energetic processes such as the detonation occurring in shock-compressed high explosives. These PVT relations of various forms of HE's (including unreacted and reacting HE's and detonation products) are also inputs to all hydrodynamics simulations of conventional and nuclear HE systems needed in every spatial and time steps. The EOS data for unreacted high explosives (UHE's) in particular are required to describe non-ideal detonation, to develop kinetic models, and to understand the safety and sensitivity of HE's and HE systems in various aging stages.

High-pressure EOS data are typically developed from Hugoniots measured in shock-wave experiments and/or isotherms in static high-pressure experiments at various temperatures. However, because of high reactivities of shock-compressed HE, it is difficult to obtain the EOS and structural information of unreacted high explosives at high pressures. In fact, it is not clear even at low pressures if there is any low level of chemical reaction occurring in shock-compressed HE. On the other hand, energetic molecules are mostly made of low-Z elements such as hydrogen, carbon, nitrogen, oxygen, which limit the application of conventional x-ray techniques to determine the PVT relation of HE in a small volume at high static pressures. For these reasons, there are very limited data available for unreacted systems mostly at low pressures below 10 GPa.[1]

Recent developments of diamond-anvil cell (DAC) technologies coupled with an intense μm-beam synchrotron x-ray are now capable of probing detailed crystal structural information from minute samples (less than 1 μg) of low-Z materials at high pressures and temperatures.[2] Therefore, in this study we have developed a DAC angle-resolved x-ray diffraction technique using monochromatic synchrotron x-ray and highly sensitive image-plate detectors.[3] This technique is capable of determining EOS and crystal structures of UHE's at high pressures above Chapmann-Jouguet (CJ) conditions. In this paper, we briefly describe the experimental method and present the EOS data of a few selected UHE's including HMX, RDX, and PETN. We will also show a few cases of applications of these data to develop the EOS and kinetic models for paste high explosives of XTX-8003 and LX-04.

ANGLE-RESOLVED SYNCHROTRON X-RAY DIFFRACTION OF HIGH EXPLOSIVE IN A DIAMOND-ANVIL HIGH-PRESSURE CELL

Diamond-anvil cell has been newly designed to obtain full circles of Debye-Sherrer's diffraction rings up to $4\Theta = 65$ degrees. By using 300 μm diamond-anvils, the cell is capable of achieving 100 GPa, well above CJ pressures of most HE ranging from 10 to 30 GPa. Powder crystals of HE samples were loaded into a 100-120 μm sample chamber drilled on a rhenium gasket with or without a pressure medium of argon (Ar). The pressure of the sample was determined from the Ruby luminescence technique.

X-ray diffraction patterns of the sample were angle-resolved on an image-plate (20x40 cm^2, Fuji), using focused, monochromatic x-ray at 20 keV from Si(111) double-crystals of the BL 10-2 at Stanford Synchrotron Radiation Laboratory (SSRL). The x-ray beam is first selected to 500 μm by 300 μm by two pairs of W-slits and is further collimated by a small micro-collimator (~30 μm, Rigaku) at approximately 30 mm apart from the sample. Considering the divergence of the beam, 2.3 mrad, it provides a gasket free diffraction pattern from the sample greater than 90 μm in diameter. The exposed imaging plate was read by a scanner (BAS-2500, Fuji) at a 100 μm resolution, and concentric Debye-Sherrer's diffraction rings were then integrated into an intensity vs. 2Θ by using a modified NIH image processing program. The image plate was placed approximately 20 cm from the sample, which recorded the angle-resolved diffraction up to 4Θ=65. The distance from the sample to the image plate was calibrated either by taking two images at two locations separated by a known distance (typically 15 cm) or by using an internal x-ray standard. Additional information for DAC angle-resolved x-ray experiments can be found elsewhere.[3]

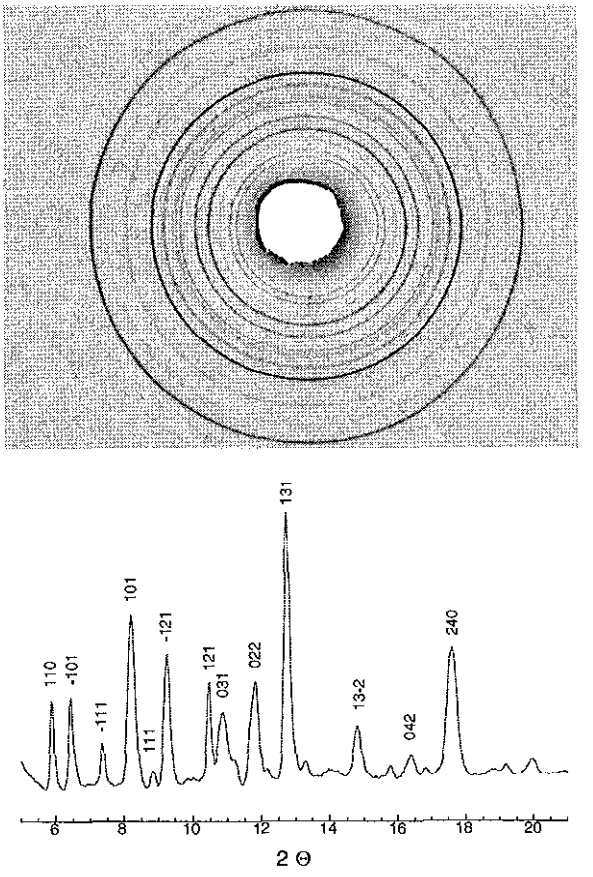

FIGURE 1. ANGLE-RESOLVED X-RAY DIFFRACTION PATTERN OF β-HMX AT 2 GPa (A: UPPER) AS RECORDED ON AN IMAGE-PLATE AFTER REMOVING THE STRUCTURELESS BACK GROUND (B: BOTTOM) AFTER INTEGRATION OF THE COCENTRIC DEBYE-SHERRER'S RINGS IN (A). INDICES FOR VARIOUS HKL LATTICE PLANES ARE BASED ON A MONOCLINIC CRYSTAL STRUCTURE.

Typical angle-resolved x-ray diffraction of β-HMX at 2 GPa is shown in Fig 1, after removing structureless back ground. The concentric rings in (a) represent Debye-Sherrer's diffraction rings from various hkl planes between 2Θ=0 and 30 degrees. The angle-resolved x-ray diffraction of β-HMX in (b) is then obtained by integrating the concentric Debye-Sherrer's rings. The lattice parameters and volumes of the sample are then determined by fitting the peak positions to various crystal structures such as the monoclinic structure of β-HMX with the space group of $P2_1/c$.[4]

HMX ISOTHERM

HMX experiments have been performed in both quasi-hydrostatic and non-hydrostatic conditions. Argon was used as a pressure medium in quasi-hydrostatic (or, "hydrostatic" hereafter for simplicity) experiments, whereas no pressure medium was used in non-hydrostatic experiments.

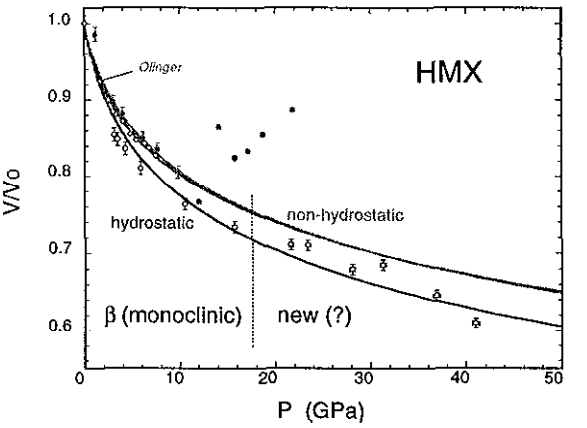

FIGURE 2. ISOTHERMS OF HMX AT THE AMBIENT TEMPERATURE IN HYDROSTATIC AND NON-HYDROSTATIC CONDITIONS.

Figure 2 presents the compression curves of HMX to 42 GPa, showing a strong dependence on the stress conditions. In hydrostatic conditions, HMX can be compressed to 42 GPa, reversibly without any apparent chemical changes. There are some scattering in the data particularly above 15 GPa, which might be due to a phase transition. On the other hand, in non-hydrostatic conditions, HMX can be compressed only to 10 GPa above which the compression data become unrealistic. The compression data below 10 GPa, however, are in

good agreement with the previous measurements by Olinger *et al.*[1] obtained using a WC-Bridgman anvil technique. Those previous WC experiments were done in a methanol-ethanol pressure medium; however, it is still close to a non-hydrostatic condition in relative to a hydrostatic condition provided by using Ar pressure medium. For example, the bulk modulus (or, stiffness) of Ar is about 1.4 GPa, substantially smaller than that of methanol, ethanol, or any other covalently-bonded hydrocarbons ranging from 10 to 20 GPa.[5] In fact, the stiffness of most HE's is also within a similar range, 10-20 GPa. Consequently, the shear strength of Ar is also expected to be smaller, providing a better hydrostatic condition.

The isotherms have been fitted to the 3rd-order Birch Murnaghan (BM) equation-of-state,[6]

$$P\,(GPa) = B_o^{3/2}\,[\,\eta^{-7/3} - \eta^{-5/3}][1 - 3\,(1 - B'/4)\,(\eta^{-2/3} - 1)]$$

where $\eta = V/V_o$ and B_o and B' are respectively the bulk modulus and its pressure derivative. The best fits were obtained with

B_o = 12.4 GPa , B' = 10.4 (in hydrostatic)
B_o = 14.4 GPa , B' = 13.3 (in non-hydrostatic)

This result is illustrated as the solid lines in Fig 2. The fits are generally good at low pressures below 10 GPa for the non-hydrostatic data and 15 GPa for the hydrostatic data. The scattering in the hydrostatic data above 15 GPa might be due to a phase transition based on our Raman studies in HMX exhibiting an indication of a conformational phase transition above 15 GPa.[7]

Note that at a given volume the hydrostatic pressure is lower than the non-hydrostatic one in Fig 1. This is quite unusual, suggesting that the difference between the hydrostatic and non-hydrostatic results can not be explained in terms of a shear-induced compression change. This unusual compression behavior of HMX in non-hydrostatic conditions is probably due to chemical reaction occurring clearly above 10 GPa or likely even below. In fact, our Raman studies of HMX[7] indicate a similar irreversible spectral change and laser-induced fluorescence in non-hydrostatic conditions, even well below 10 GPa. In contrast, all the spectral changes of HMX in hydrostatic conditions are reversible and no fluorescence is apparent at all pressures to 45 GPa. Therefore, we conclude that the abnormal compression behavior in non-hydrostatic conditions is due to exothermic chemical reactions which should increase the pressure above the hydrostatic value at a given confined volume of unreacted HMX. Similar exothermic chemical reactions (or, "detonation") have previously been observed in unaxially compressed nitromethane[8] and cubanes[9] in DAC experiments. It has also been suggested that the sensitivity of such a reaction is crystal orientation dependent with respect to the applied stress in a DAC.

The results of HMX experiments clearly indicate the importance of shear-induced chemical reaction in non-hydrostatic conditions. Further systematic studies are currently underway to correlate the shear-induced chemistry to the changes in HMX crystal structures at high pressures. The results associated with HMX crystal structures and phase transition will be reported elsewhere.[7]

RDX ISOTHERM

RDX experiments have been done only in hydrostatic Ar pressure medium. However, the results have been compared with the previous WC-anvil experiments, again, representing somewhat higher non-hydrostaticity. The diffraction patterns were indexed based on an orthorhombic structure by using more than 15 diffraction planes between 111 at $2\Theta=5.5^0$ and 322 at 13^0. It is well known that RDX-I (orthorhombic with Pbca space group)[10] undergoes a phase transition to RDX-III at about 4 GPa.[1] This phase transition has been proposed to be conformational, which retains its basic crystallographic symmetry but alters its molecular structure. Therefore, in this study we have used a same orthorhombic symmetry to fit the data at all pressures.

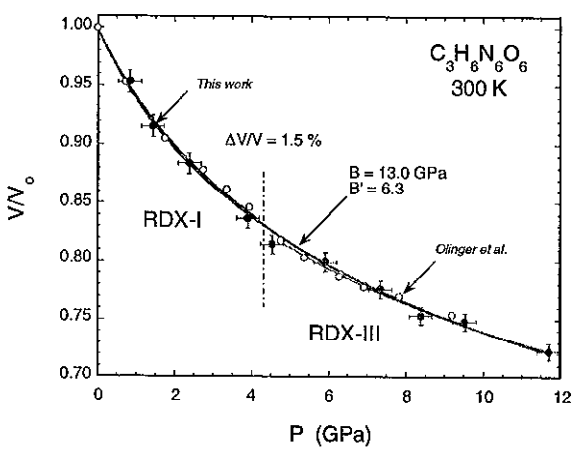

FIGURE 3. ISOTHERMS OF RDX IN Ar TO 12 GPa (SOLID CIRCLES WITH ERROR BARS) AT THE AMBIENT TEMPERATURE IN COMPARISON WITH THE PREVIOUS WC-MEASUREMENTS (OPEN CIRCLES WITHOUT ERROR BARS).

The compression data are summarized in Fig 3, together with the previous WC results. These compression data agree very well, clearly suggesting no stress dependent behavior of RDX. It is in contrast to the case of HMX, despite their chemical similarity. The

differences in crystal structures and shear-plane interactions may result such a difference in compression curves of RDX and HMX.

The compression data have been fitted to the BM-EOS, resulting in B_o and B' of

B_o = 13.9 GPa , B' = 5.8 (RDX-I)
B_o = 10.9 GPa , B' = 7.9 (RDX-III)
B_o = 13.0 GPa , B' = 6.3 (overall)

These fits shown as the solid lines in Fig 3 are extremely good as seen in Fig 3. The results also yield a small, but apparent discontinuous volume change at 4.2 GPa, which we attribute to the phase transition from RDX-I to RDX-III. The transition volume change is then found to be 1.5 %. This is in very good agreement with the previous WC-result, 1.6 %.[1] The consistency in compression data of two different phases and a small transition volume change support that the transition is indeed a conformational one. Furthermore, our preliminary Rietveld analysis also indicates that the structure of RDX-III is orthorhombic with a likely space group of Pm2a or Pcca. Detailed analysis of the crystal structure of RDX-III is currently underway and will be reported later.

PETN ISOTHERM

PETN experiments have been done in hydrostatic Ar pressure medium. There have been no previously reported compression data of PETN in static high pressure conditions. This is in part due to highly preferred orientation of PETN crystals at high pressures as shown in Fig 4.

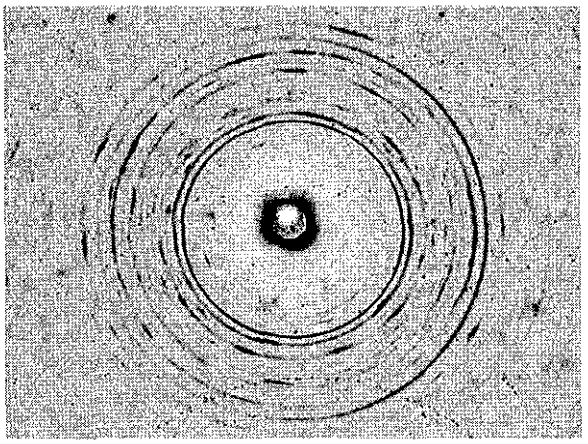

FIGURE 4. AN IMAGE-PLATE RECORD OF PETN IN Ar AT 3.2 GPa AFTER REMOVING STRUCTURELESS BACKGROUND SHOWING HIGHLY PREFERRED ORIENTATION.

Clearly, the spotty nature of PETN diffraction is quite distinctive to those of HMX and RDX, emphasizing the importance of obtaining full-circles of Debye-Sherrer's diffraction rings in order to accurately determine the crystal structure of PETN at high pressures. On the other hand, PETN is notorious to show very strong crystallographic anisotropy in its detonation behavior under shock compression.[11,12] However, it has not been explored as yet if there is any relationship between the preferred orientation and the anisotropic behavior of crystals.

By integrating the concentric rings of Fig 4, it is feasible to identify 10 diffraction planes of 201, 002, 221, 200, 201, 121, 220, 102, 301, 311, and to confirm the crystal structure of PETN to be orthorhombic with $P2_12_1$ space group consistent with the previous result.[13] The resulted volume data are presented in Fig 5 (as solid circles with error bars), together with the previously reported Hugoniot data of PETN single crystals.[14] The solid and dotted lines represent the BM-EOS fits to this static and previous shock data, respectively. Clearly, these fits are in good agreement with the experiments, yielding

B_o = 12.3 GPa , B' = 8.2 (Isotherm)
B_o = 11.8 GPa , B' = 9.1 (Hugoniot)

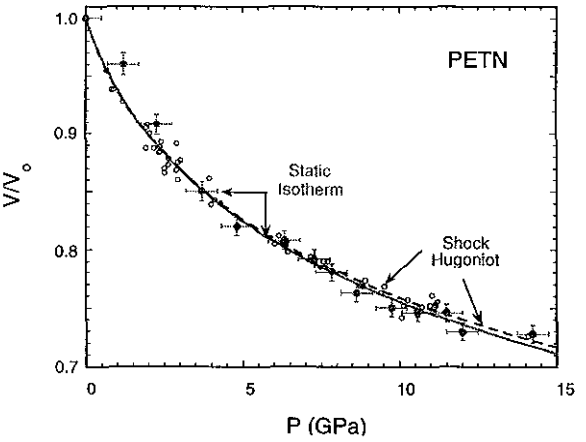

FIGURE 5. STATIC ISOTHERM OF PETN IN Ar TO 15 GPa AT THE AMBIENT TEMPERATURE IN COMPARISON WITH SHOCK HUGONIOT OF SINGLE CRYSTAL PETN.

There is very good agreement between the static-isotherm and the shock-Hugoniot in Fig 5. The difference is, in fact, smaller than the uncertainties of the fits or in the data. A slight increase in volume of shock Hugoniot above 10 GPa, however, may reflect a small temperature effect associated with shock compression, which remains to be small within the pressure range of this study,

APPLICATIONS OF THE EOS OF UHE DATA TO KINETIC AND EOS MODELS FOR HE COMPOSITES

In this section, we will show how these data are used to develop EOS, detonation, and kinetic models for composite HE's. The detonation velocity of a high explosive is usually calculated in a thermochemical code with the assumption of full chemical and thermal equilibrium for the product gases. This also assumes that all of the high explosive and binder are consumed in the detonation wave. However, so called "non-ideal" explosives with finite reaction zones do not always achieve instantaneous chemical equilibrium and combust all of their fuel in the detonation wave, for which case one would need the UHE information to describe its kinetics.

We first show the application of the equation of state data reported here for unburned HMX (the hydrostatic value) and PETN. The values for B_o and B' are used to calculate an unburned EOS for HE composites and compare the results with shock velocity versus particle velocity (U_s vs. U_p) relations determined from previous shock-wave experiments.[15,16] In this calculation, we use a multiphase EOS model of gases and condensed solids, for which we use the Mie-Gruneisen EOS to evaluate an appropriate thermal contribution.[17] Two composites have been compared in this study, XTX-8003 and LX-04. The compositions of these composites are given in Table 1.

TABLE 1. COMPOSITIONS OF HE COMPOSITES.

Composite	Composition (by weight)
XTX-8003	PETN, 80%, SYLGARD, 20%
LX-04	HMX, 85%, VITON, 15%

Figure 6 shows the calculated (solid line) and experimental (solid triangles)[15] U_s-U_p relation for XTX-8003. The highest experimental point corresponds to a pressure of about 5 GPa; at this point a significant deviation from the calculation begins to occur. This deviation may be due to having too soft an EOS for the binder. To clarify this issue, we may also need the EOS for the binder materials, which will be determined in later studies. Figure 7 shows the calculated (dashed line) and experimental (solid line)[16] $U_s - U_p$ relation for LX-04. The data is assumed valid to about 43 GPa (U_s = 3.24 km/s), where the agreement with the calculation is excellent.

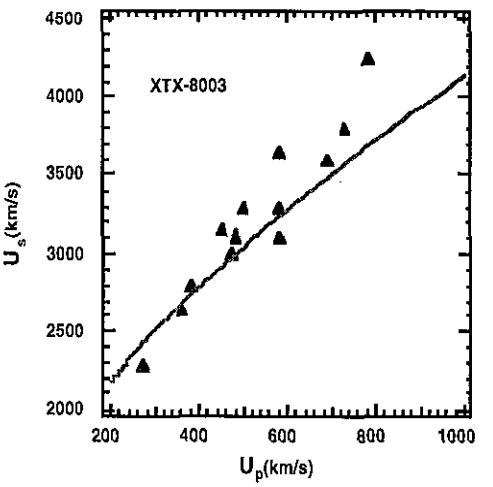

FIGURE 6. CALCULATED (SOLID LINE) AND EXPERIMENTAL (SOLID TRIANGLES) U_S-U_P RELATION OF UNBURNED XTX-8003.

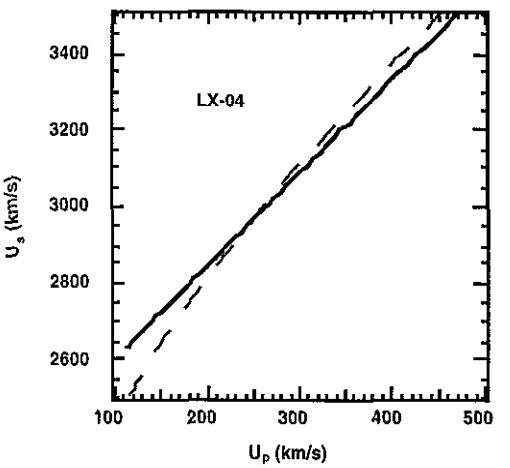

FIGURE 7. CALCULATED (DASHED LINE) AND EXPERIMENTAL (SOLID LINE) U_S-U_P RELATION FOR UNBURNED LX-04.

Now we apply these EOS's of UHE's to developing kinetic models of the detonation in HE composites. We use an implementation of the Wood-Kirkwood[18,19] (WK) kinetic detonation model based on multi-species equations of state and multiple reaction rate laws. Such a model requires equations of state for the unburned composites, and a kinetic rate law model for their decomposition. We model the kinetic processes of the high explosives and binders as being a single decomposition reaction into primary product constituents. With such a model we find that we can replicate experimental detonation velocities for a wide range of ideal and non-ideal explosives.[17] We have inferred effective kinetic rates proportional to P^2 for a variety of ideal and non-ideal explosives and their

composites. In the following we show some results for a kinetic calculation for LX-04.

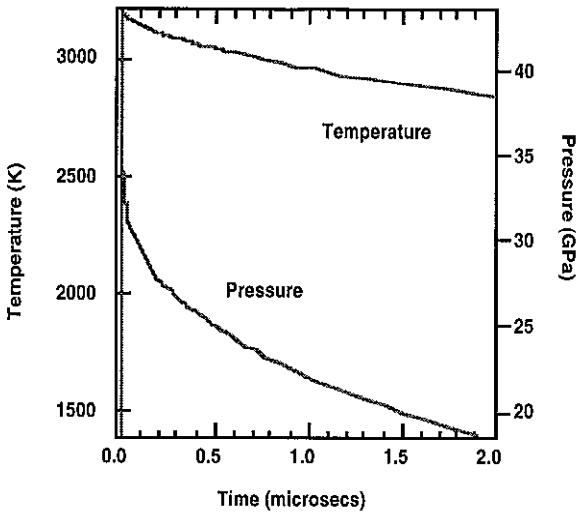

FIGURE 8. TIME VARIATION OF THE PRESSURE AND TEMPERATURE FOR A KINETIC CALCULATION OF LX-04.

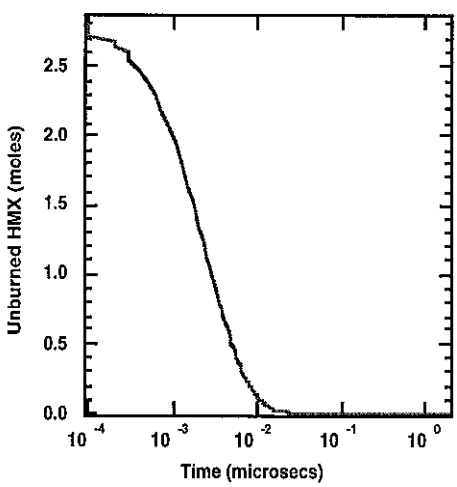

FIGURE 9. UNBURNED HMX AS A FUNCTION OF TIME FOR A KINETIC LX-04 CALCULATION.

Figures 8 and 9 show the time dependence of the pressure, temperature and HMX concentration in the detonation of LX-04. For the case of kinetic calculations, temperature and pressure are followed from the completely unreacted state to the completely decomposed state as seen in Fig 8. For this case, all of the HMX decomposition energy contributes to detonation wave, which processes strongly depends on the EOS's of UHE's. The time scale for the HMX decomposition seen in Fig 9 is determined from the study of many ideal and non-ideal HE composites, which also require the EOS for non-reacted HE as an input.[15]

In these studies it is still difficult to differentiate some kinetic effects from equation of state effects. Therefore, development of realistic equations of state for unburned high explosives and binders is absolutely essential for the development of kinetic models of thermochemical detonations. We certainly need more data for high explosives and binders at high pressure. Such kinetic models are useful for predicting the features of non-ideal explosives such as their detonation velocities and their sonic reaction zones width.

CONCLUDING REMARKS

In this study, we have demonstrated the feasibility of obtaining reliable sets of EOS data for unreacted high explosives at very high pressures well beyond the CJ conditions, by using a DAC angle-resolved synchrotron x-ray diffraction technique. The compression data and EOS parameters (*ie*, B_0 and B') of UHE have been determined for HMX to 42 GPa, RDX to 12 GPa, PETN to 15 GPa at the ambient temperature. These EOS data of UHE's are, of course, fundamental to developing both EOS and kinetic models of various HE systems and HE composites, in various stages of non-ideal detonation such as the combustion, deflagration, decomposition, partial detonation, degradation, and HE agings. Two examples of such applications have been shown for developing the EOS and kinetic models of LX-04 and XTX-8003 based on the measured EOS's of HMX and PETN, respectively. The crystal structure information of the x-ray data, on the other hand, provides the insight to the high-pressure behavior of UHE's such as the phase transitions in HMX and RDX, shear-induced chemistry of HMX, and mechanical anisotropic responses of PETN crystals and sensitivity.

ACKNOWLEDGMENTS

The synchrotron x-ray work reported here has been done at the SSRL. We appreciate Dr. Pagoria for providing HE samples used in this study, and the technical discussions with Drs. Ree, Fried, and Souers, were very productive for this study. This work was done in support of a Joint DoD/DOE Munition Technology Development Program and has been done under the auspices of the U.S. Department of Energy by the Lawrence Livermore National Laboratory under contract number W-7405-ENG-48.

REFERENCES

1. Olinger, B., Roof, R. B., and Cady, H., "The Linear and Volume Compression of b-HMX and RDX to 9 GPa (90 kilobar)" a Proceedings to Symposium H. D. P. (Commissariat a l'Energie Atomique, 1978), pp 3-8.

2. Loubeyre, P., LeToullec, R., Hausermann, D., Hanfland, M., Hemley, R.J., Mao, H.K., and Finger, L.W., "X-ray Diffraction and Equation of State of Hydrogen at Megabar Pressures", Nature 383, 1996, pp 702-1996.

3. Cynn, H., Yoo, C. S., and Sheffield, S. "Phase Transition and Decomposition of 90 % Hydrogen Peroxide at High Pressures, J. Chem. Phys., 1998, in print.

4. Choi, C. S. and Boutin, H. P.,"A Study of the Crystal Structure of β-Cyclotetramethylene Tetranitramine by Neutron Diffraction," Acta Cryst. B26, 1970, pp 1235-1240.

5. Knittle, E., "Static Compression Measurements of Equation of State" in "Mineral Physics and Crystallography, a Handbook of Physical Constants" Edited by Ahrens, T., AGU, 1995, pp 98-142.

6. Birch, F., "The Effect of Pressure Upon the Elastic Parameters of Isotropic Solids, According to Murnaghan's Theory of Finite Strain," J. Appl. Phys. 4, 1938, pp 279 - 288.

7. Yoo, C. S and H. Cynn, to be published.

8. Piermarini, G.J., Block, S., Miller, P.J., "Effects of Pressure on the Thermal Decomposition Kinetics and Chemical Reactivity of Nitromethane", J. Phys. Chem. 93, 1989, 457 - 462.

9. Piermarini, G. J., Block, S., Damavarapu, R., Iyer, S., "1,4-Dinitrocubane and Cubane under High Pressure", Propellants, Explosives, Pyrotechnics 16, 1991, 188 - 193.

10. Choi, C. S., Prince, E., "The Crystal Structure of Cyclotrimethylene-Trinitramine," Acta Cryst. B28, 1972, pp 2857-2862.

11. Dick, J. J. and Ritchie, J. P., "Molecular Mechanics Modeling of Shear and the Crystal Orientation Dependence of the Elastic Precursor Shock Strength in Pentaerythritol Tetranitrate", J. Appl. Phys. 76, 1994, pp 2726 - 2737.

12. Yoo, C. S., Holmes, N. C., and Souers, P. C., "Detonation in Shocked Homogeneous High Explosives", in "Decomposition, Combustion, and Detonation Chemistry of Energetic Materials," Edited by Brill, T. B. *et al.*, MRS vol 418, 1996, pp 397 - 405.

13. Booth, A.D., Llewellyn, S.J. "The Crystal Structure of Pentaerythritol Tetranitrate" J. Am. Chem. Soc., 1947, pp 837-846

14. Marsh, S. P., "LASL Shock Hugoniot Data" (University of California, Berkeley, 1980).

15. Stirpe, D., Johnson, J. O. and Wackerle, J., "Shock Initiation of XTX-8003 and Pressed PETN", J. Appl. Phys., **41**, 1970, pp. 3884.

16. Dobratz, B. M. and Crawford, P. C., "LLNL Explosives Handbook Properties of Chemical Explosives and Explosive Simulants", report UCRL-52997 change 2, January 31, 1985.

17. Howard, W. M. , Fried, L. E. and Souers, P. C., "Kinetic Modeling of Non-Ideal Explosives with Cheetah", 11th International Detonation Symposium, Snowmass, Co, 30 August to 4 September, 1998.

18. Wood, W. W. and Kirkwood, J. G., "Diameter Effect in Condensed Explosives", J. Chem. Phys., 22, 1954, pp. 1920-1924.

19. Fickett, W. and Davis, W. C., "Detonation", University of California Press, Berkeley, 1979, Ch. 5.